$(N_3)^{2+}$-$Eu(N_3)^{2+}$. All the pure nitrogen ligands are in the group of high S_F values. Similarly, covalent interactions are the cause of these high selection factors, since the ionic radii of Am(III) and Eu(III) (1.09 and 1.06 Å) suggest that, for pure ionic bonds, the Eu(III) complexes will be the more stable. This trend is observed in the fluoride complexes.

However, it is unlikely that the type II geometry found for $Gd(N_3)^{2+}$ arises from the presence of a covalent bond with a sp^2-hybridized nitrogen strongly linked to the metal, as in trivalent d transition azido complexes, for which β_{11} values are several orders of magnitude higher than the β_{11} of the lanthanide complexes. The N_3^- position probably results from the action of antagonistic forces. Azide negative charge density is equally shared between N_1 and N_3 nitrogens,[21] and N_3^- ions are ionically attracted by the metal and the nearest water molecules. The observed position is most probably the resultant of these two kinds of interactions.

The investigation of hexa- and tetravalent azido complexes of actinides supports these assumptions.[22] Configuration III was found in U(VI) complexes. The linearity of $M(NCS)^{2+}$ lanthanide species could also be understood from the predominantly ionic interactions, because the negative charge densities carried by sulfur and nitrogen[21] are smaller than those of N_3^- terminal nitrogen, as shown in IV and V, and the linear configuration is favored.

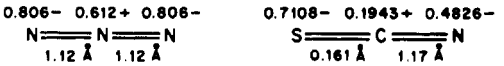

IV V

The spin density transferred from Gd(III) to N_3^- is slightly higher to the spin transferred[3] from Gd(III) to NCS^- or to the solvation water molecules[23] but is one order of magnitude lower than the spin density transferred from Co(II) to NCS^-.[24]

Acknowledgment. We are indebted to Prof. R. Guillaumont, who welcomed C. Cuillerdier into his laboratory to start the solvent-extraction investigations.

(21) S. M. Nelson, *MTP Int. Rev. Sci.: Inorg. Chem., Ser. One*, **5**, 211 (1972).

(22) C. Musikas et al., to be submitted for publication in *Inorg. Chem.*
(23) J. Reuben and D. Fiat, *J. Chem. Phys.*, **51**, 4909 (1969).
(24) A. H. Zeltmann and L. O. Morgan, *Inorg. Chem.*, **9**, 2522 (1970).

Contribution from the Institut für Physikalische und Theoretische Chemie and Physikalisches Institut, Abt. II, University of Erlangen-Nürnberg, D-8520 Erlangen, West Germany, and the School of Chemistry, University of New South Wales, Kensington, NSW 2033, Australia

Nature of the Continuous High-Spin ($^5T_2$) ⇌ Low-Spin ($^1A_1$) Transition in Bis[2-((4-methyl-2-pyridyl)amino)-4-(2-pyridyl)thiazole]iron(II) Diperchlorate Dihydrate and Bis(tetrafluoroborate) Dihydrate: Mössbauer Effect and X-ray Diffraction Study

E. KÖNIG,*[1a] G. RITTER,[1b] S. K. KULSHRESHTHA,[1a,c] and H. A. GOODWIN[2]

Received October 7, 1982

The gradual high-spin ($S = 2$, $^5T_2$) ⇌ low-spin ($S = 0$, $^1A_1$) transformations in solid $[Fe(4\text{-paptH})_2](ClO_4)_2 \cdot 2H_2O$ and $[Fe(4\text{-paptH})_2](BF_4)_2 \cdot 2H_2O$ (4-paptH = 2-((4-methyl-2-pyridyl)amino)-4-(2-pyridyl)thiazole) have been studied by variable-temperature ^{57}Fe Mössbauer effect and X-ray diffraction. For the complex perchlorate, the ground states involved are characterized, at the transition temperature $T_c \approx 185$ K, by the quadrupole splitting $\Delta E_Q(^5T_2) = 2.40$ mm s^{-1}, $\Delta E_Q(^1A_1) = 1.31$ mm s^{-1} and the isomer shift $\delta^{IS}(^5T_2) = +1.05$ mm s^{-1}, $\delta^{IS}(^1A_1) = +0.42$ mm s^{-1}. For the complex tetrafluoroborate, the corresponding values at the transition temperature $T_c \approx 220$ K are $\Delta E_Q(^5T_2) = 2.40$ mm s^{-1}, $\Delta E_Q(^1A_1) = 1.32$ mm s^{-1} and $\delta^{IS}(^5T_2) = +1.01$ mm s^{-1}, $\delta^{IS}(^1A_1) = +0.39$ mm s^{-1}. The observed nonlinear temperature dependence of $-\ln(\sum t_i)$, where t_i is the effective thickness ($i = {}^5T_2, {}^1A_1$), is consistent with different Debye-Waller factors, $-\ln f_{^5T_2}$ and $-\ln f_{^1A_1}$. The same conclusion is indicated by the observation of different temperature factors for the isomer shift. The lattice spacings derived from X-ray diffraction show a continuous variation with temperature which parallels that of the $^5T_2$ fraction, $n_{^5T_2}$. The results are interpreted in terms of the formation of a solid solution of the two spin isomers within the one lattice. The continuous character of the transition is consistent with the assumption of weak cooperative interaction between the individual complexes and a wide distribution of the nuclei of the minority constituent.

Introduction

The discontinuous type high-spin ($^5T_2$) ⇌ low-spin ($^1A_1$) transitions in solid compounds of iron(II) now seem to be reasonably well understood. Such transitions arise for compounds with a strong cooperative interaction between the individual complexes. In the transition region, pronounced domain formation by both minority and majority phases is encountered, and thus individual X-ray diffraction patterns for the two phases are observed. Due to the interaction, a crystallographic phase change is, in general, involved. Hysteresis effects, if present, are a consequence of the domain formation. To date, consistent results have been derived from the temperature dependence of X-ray diffraction and Mössbauer effect data for a number of systems, i.e. for $[Fe(phy)_2](ClO_4)_2$ (where phy = 1,10-phenanthroline-2-carbaldehyde phenylhydrazone),[3] $[Fe(bt)_2(NCS)_2]$ (where bt = 2,2′-bi-2-thiazoline),[4] $[Fe(4,7\text{-}(CH_3)_2phen)_2(NCS)_2]$ (where 4,7-$(CH_3)_2$phen = 4,7-dimethyl-1,10-phenanthroline),[5] and $[Fe(bi)_3](ClO_4)_2$ (where bi = 2,2′-bi-2-imidazoline).[6] It thus seems that the conclusions are of general applicability to spin transitions of the discontinuous type.

(1) (a) Institut für Physikalische und Theoretische Chemie, University of Erlangen-Nürnberg. (b) Physikalisches Institut, Abt. II, University of Erlangen-Nürnberg. (c) On leave of absence from the Chemistry Division, Bhabha Atomic Research Centre, Bombay, India.
(2) University of New South Wales.

(3) König, E.; Ritter, G.; Irler, W.; Goodwin, H. A. *J. Am. Chem. Soc.* **1980**, *102*, 4681.
(4) König, E.; Ritter, G.; Irler, W.; Nelson, S. M. *Inorg. Chim. Acta* **1979**, *37*, 169.
(5) König, E.; Ritter, G.; Irler, W. *Chem. Phys. Lett.* **1979**, *66*, 336.
(6) König, E.; Ritter, G.; Kulshreshtha, S. K.; Nelson, S. M. *Inorg. Chem.* **1982**, *21*, 3022.

0020-1669/83/1322-2518$01.50/0

The change of a discontinuous type of transition, when the sample is ground or doped,[7-9] into a transition showing a quasi-continuous behavior is a consequence of the smaller size of the crystallites that are formed. Thus, the cooperative process will be terminated after a much shorter distance than in the original sample and this will result in a decreased size of domains and a more gradual appearance of the transition. Nevertheless, the essential features of the first-order transition such as hystersis effects are retained.[3,9] On the other hand, if, on recrystallization, larger size crystallites are formed, the change of a quasi-continuous transition into that of a discontinuous type may be observed.[3]

The rationalization of the continuous type high-spin ($^5T_2$) ⇌ low-spin ($^1A_1$) transitions has, however, proved more difficult. In a recent investigation of the gradual transition in $[Fe(bts)_2(NCS)_2]$, where bts = 2,2'-bi(5-methyl-2-thiazoline), we have shown[10] that, in the transition region, no individual X-ray diffraction patterns for the two constituents having different spin states are found. Rather, the interplanar spacings d_{hkl} derived from X-ray diffraction show a continuous variation with temperature which parallels that of the high-spin fraction, $n_{^5T_2}$. The observation has been interpreted by the formation of a random solid solution of the two spin isomers within the same lattice. The continuous character of the transition is consistent with weak cooperative interaction between the individual complexes and a wide distribution of the nuclei of the minority constituent. It is obviously of importance to consider further systems that display gradual transitions in order to test the generality of the above interpretations.

Continuous high-spin ($^5T_2$) ⇌ low-spin ($^1A_1$) transitions have been reported for a number of iron(II) complexes of the heterocyclic ligands 2-((3-methyl-2-pyridyl)amino)- and 2-((4-methyl-2-pyridyl)amino)-4-(2-pyridyl)thiazole.[11] The interpretation of the results has been based essentially on the temperature dependence of the magnetic properties. In the present contribution, we report, therefore, a more detailed analysis of the spin transition in the compounds $[Fe(4\text{-}paptH)_2](ClO_4)_2\cdot 2H_2O$ and $[Fe(4\text{-}paptH)_2](BF_4)_2\cdot 2H_2O$ based on ^{57}Fe Mössbauer-effect and X-ray powder diffraction measurements (4-paptH = 2-((4-methyl-2-pyridyl)amino)-4-(2-pyridyl)thiazole).

Experimental Section

Materials. The ligand and the tetrafluoroborate complex $[Fe(4\text{-}paptH)_2](BF_4)_2\cdot 2H_2O$ were prepared as described elsewhere.[11,12] The perchlorate complex $[Fe(4\text{-}paptH)_2](ClO_4)_2\cdot 2H_2O$ was obtained by a method essentially the same as that for the tetrafluoroborate except that sodium perchlorate was used as the additive. Both compounds gave satisfactory analyses, their physical data being consistent with those previously reported.[11] In addition, the retention of the hydrate water during pumping in the course of the X-ray diffraction study described below has been confirmed by elemental analysis.

Methods. ^{57}Fe Mössbauer spectra were measured as described in detail in our previous reports.[3,6] All velocity scales and isomer shifts are referred to a metallic iron standard at 298 K. To convert to the sodium nitroprusside scale, add +0.257 mm s^{-1}. The individual areas A_i were extracted from the background-corrected data by a computer-based decomposition into Lorentzians. The effective thickness t_i of an individual peak is defined by the relation

$$A_i = \frac{1}{2}\pi\Gamma f_S \frac{t_i}{1 + 0.25t_i} \qquad (1)$$

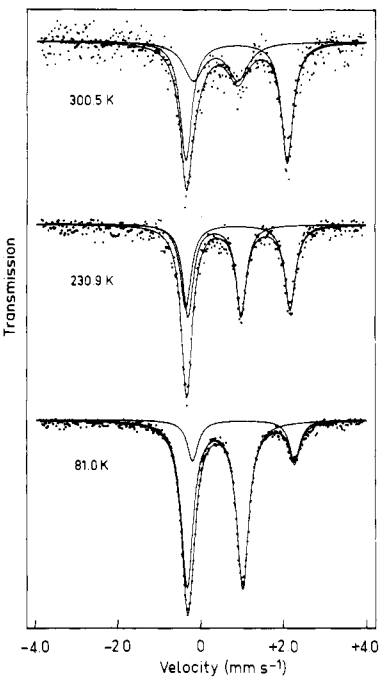

Figure 1. ^{57}Fe Mössbauer spectra of $[Fe(4\text{-}paptH)_2](ClO_4)_2\cdot 2H_2O$ at 81.0, 230.9, and 300.5 K measured for increasing temperatures. The transition is centered at $T_c \approx 185$ K.

Here, $^1/_2\pi\Gamma f_S$ is a scaling factor which is determined from the spectra of standard materials, the individual quantities having been defined elsewhere.[3,6] The effective thicknesses for the two constituents of different spin, $t_{^5T_2}$ and $t_{^1A_1}$, which are sums of their individual component values t_i are also given by

$$t_{^5T_2} = dn_{^5T_2}f_{^5T_2} \qquad t_{^1A_1} = d(1 - n_{^5T_2})f_{^1A_1} \qquad (2)$$

In eq 2, $n_{^5T_2}$ is the high-spin fraction, $f_{^5T_2}$ and $f_{^1A_1}$ are the recoilfree fractions for the two phases, and $d = N\beta\delta\sigma_0$, the quantities involved having the usual meaning.[6]

Magnetic susceptibilities were determined according to the Gouy method with a Newport Instruments variable-temperature magnetic balance.

Measurements of X-ray powder diffraction were performed in the mode of step scanning of the diffractometer, the step being 0.02° in 2θ. The resulting pulses were stored and processed by a multichannel analyzer. More details on the equipment and the method employed have been given previously.[3,6]

Results

^{57}Fe Mössbauer Effect. The sample of $[Fe(4\text{-}paptH)_2](ClO_4)_2\cdot H_2O$ has been studied between 81.0 and 300.5 K. Figure 1 shows three typical spectra, i.e. those collected at 81.0, 230.9, and 300.5 K. The decomposition into Lorentzians shows that the spectrum at 81.0 K consists of two overlapping doublets. The more intense doublet is characterized by the quadrupole splitting $\Delta E_Q = 1.31 \pm 0.04$ mm s^{-1} and the isomer shift $\delta^{IS} = +0.44 \pm 0.02$ mm s^{-1} and is assigned to the low-spin $^1A_1$ ground state of iron(II). The less intense doublet yields $\Delta E_Q = 2.41 \pm 0.04$ mm s^{-1} and $\delta^{IS} = +1.11 \pm 0.02$ mm s^{-1} and is attributed to the high-spin $^5T_2$ ground state of iron(II). With increasing temperature, the $^5T_2$ doublet gains intensity, while the intensity of the $^1A_1$ doublet simultaneously decreases. At about 230.9 K, the intensities of the two spectra appear almost equal and, at 300.5 K, the contribution of the $^5T_2$ doublet is clearly predominant. At this temperature, the $^5T_2$ doublet is characterized by $\Delta E_Q = 2.40 \pm 0.04$ mm s^{-1} and $\delta^{IS} = +0.94 \pm 0.02$ mm s^{-1}. The detailed values of the Mössbauer parameters including the relative effective thickness $t_{^5T_2}/t_{total}$ are listed in Table I for a representative set of temperatures. It is evident that a high-spin ($^5T_2$) ⇌ low-spin ($^1A_1$) transition is induced in $[Fe(4\text{-}paptH)_2](ClO_4)_2\cdot 2H_2O$ by the

(7) Haddad, M. S.; Federer, W. D.; Lynch, M. W.; Hendrickson, D. N. *Inorg. Chem.* **1981**, *20*, 131.
(8) Haddad, M. S.; Lynch, M. W.; Federer, W. D.; Hendrickson, D. N. *Inorg. Chem.* **1981**, *20*, 123.
(9) König, E.; Ritter, G.; Kulshreshtha, S. K.; Csatary, N., to be submitted for publication.
(10) König, E.; Ritter, G.; Kulshreshtha, S. K.; Nelson, S. M. *J. Am. Chem. Soc.* **1983**, *105*, 1924.
(11) Goodwin, H. A.; Mather, D. W. *Aust. J. Chem.* **1972**, *25*, 715.
(12) Goodwin, H. A. *Aust. J. Chem.* **1964**, *17*, 1366.

Table I. ^{57}Fe Mössbauer-Effect Parameters of $[Fe(4\text{-}paptH)_2](ClO_4)_2 \cdot 2H_2O$ for a Set of Representative Temperatures

T, K	$\Delta E_Q(^1A_1)$,[a] mm s^{-1}	$\delta^{IS}(^1A_1)$,[b] mm s^{-1}	$\Delta E_Q(^5T_2)$,[a] mm s^{-1}	$\delta^{IS}(^5T_2)$,[b] mm s^{-1}	$t_{^5T_2}/t_{total}$
81.0	1.31	+0.44	2.41	+1.11	0.170
104.3	1.31	+0.43	2.41	+1.10	0.183
133.3	1.31	+0.43	2.42	+1.08	0.201
161.8	1.31	+0.42	2.42	+1.06	0.283
178.0	1.31	+0.42	2.40	+1.05	0.316
194.3	1.30	+0.42	2.43	+1.02	0.378
210.9	1.31	+0.41	2.41	+1.01	0.431
230.9	1.26	+0.42	2.47	+0.97	0.492
238.1	1.29	+0.40	2.47	+0.98	0.498
258.1	1.32	+0.39	2.37	+0.98	0.605
277.4	1.29	+0.36	2.39	+0.96	0.654
287.2	1.10 ± 0.10	+0.43 ± 0.05	2.41	+0.94	0.663
300.5	1.06 ± 0.10	+0.44 ± 0.06	2.40	+0.94	0.654

[a] The experimental uncertainty is ±0.04 mm s^{-1} except where stated. [b] Isomer shifts δ^{IS} are listed relative to natural iron at 298 K. The experimental uncertainty is ±0.02 mm s^{-1} except where stated.

Table II. ^{57}Fe Mössbauer-Effect Parameters of $[Fe(4\text{-}paptH)_2](BF_4)_2 \cdot 2H_2O$ for a Set of Representative Temperatures

T, K	$\Delta E_Q(^1A_1)$,[a] mm s^{-1}	$\delta^{IS}(^1A_1)$,[b] mm s^{-1}	$\Delta E_Q(^5T_2)$,[a] mm s^{-1}	$\delta^{IS}(^5T_2)$,[b] mm s^{-1}	$t_{^5T_2}/t_{total}$
80.4	1.31	+0.44	2.42	+1.11	0.160
95.0	1.31	+0.44	2.44	+1.11	0.169
128.9	1.31	+0.43	2.42	+1.09	0.199
148.4	1.31	+0.42	2.42	+1.07	0.243
176.5	1.32	+0.41	2.40	+1.05	0.285
190.5	1.32	+0.41	2.39	+1.04	0.323
206.3	1.32	+0.40	2.42	+1.03	0.346
219.4	1.32	+0.39	2.40	+1.01	0.380
233.7	1.32	+0.39	2.41	+1.00	0.417
248.5	1.32	+0.36	2.38	+0.99	0.499
272.6	1.31	+0.37	2.38	+0.98	0.578
287.2	1.12 ± 0.10	+0.40 ± 0.05	2.31	+0.93	0.641
293.6	1.11 ± 0.10	+0.41 ± 0.05	2.31	+0.93	0.612
301.8	0.99 ± 0.10	+0.42 ± 0.05	2.31	+0.93	0.638

[a] The experimental uncertainty is ±0.04 mm s^{-1} except where stated. [b] Isomer shifts δ^{IS} are listed relative to natural iron at 298 K. The experimental uncertainty is ±0.02 mm s^{-1} except where stated.

temperature change. The transition is of the continuous type and is incomplete at both the low- and the high-temperature limits of the measurements. This may be clearly demonstrated by the values of $t_{^5T_2}/t_{total}$, which qualitatively represent the behavior of the high-spin fraction $n_{^5T_2}$, if the difference in the recoil-free fraction of the two spin constituents is neglected. Thus, at 81.0 K, $t_{^5T_2}/t_{total} = 0.170$, whereas at 300.5 K, $t_{^5T_2}/t_{total} = 0.654$ (cf. Table I). We have verified that the residual $^5T_2$ fraction obtained at 81.0 K remains almost unchanged even at 4.2 K. The sample was studied for both increasing and decreasing temperatures with practically identical results, and no hysteresis effects have been encountered. Altogether, spectra at 28 temperatures have been collected.

The sample of $[Fe(4\text{-}paptH)_2](BF_4)_2 \cdot 2H_2O$ has been studied between 80.4 and 301.8 K, three typical spectra, i.e. at 293.6, 248.5, and 80.4 K, being displayed in Figure 2.

The detailed values of the Mössbauer parameters are listed in Table II for a representative set of temperatures. It is obvious that the behavior of the tetrafluoroborate is closely similar to that of the perchlorate. Again, the transition is of the continuous type with appreciable residual fractions by both the $^5T_2$ and the $^1A_1$ state at the low- and the high-temperature end, respectively. At 4.2 K, practically the same value for $t_{^5T_2}/t_{total}$ has been obtained as at 80.4 K. Altogether, spectra at 28 different temperatures have been measured in decreasing

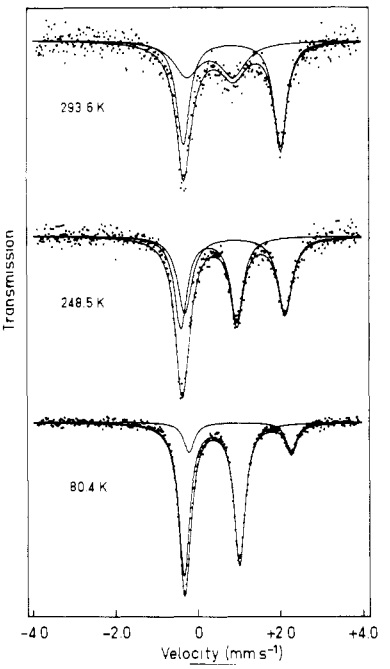

Figure 2. ^{57}Fe Mössbauer spectra of $[Fe(4\text{-}paptH)_2](BF_4)_2 \cdot 2H_2O$ at 80.4, 248.5, and 293.6 K measured for decreasing temperatures. The transition is centered at $T_c \approx 220$ K.

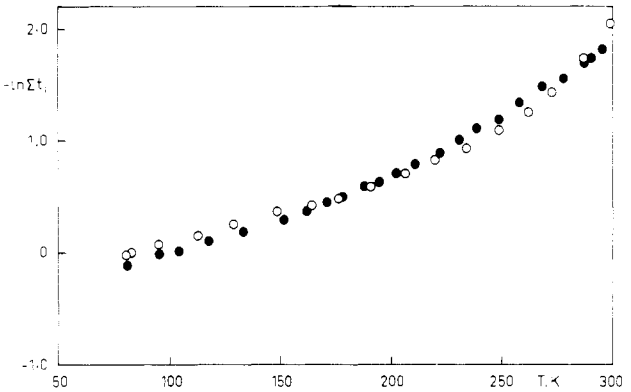

Figure 3. Temperature dependence of the quantity $-\ln(\sum t_i)$, i = $^5T_2$, $^1A_1$, where t_i is the effective thickness, for $[Fe(4\text{-}paptH)_2](ClO_4)_2 \cdot 2H_2O$ (●) for increasing temperatures and for $[Fe(4\text{-}paptH)_2](BF_4)_2 \cdot 2H_2O$ (○) for decreasing temperatures.

and increasing temperature sequence, and no hystersis effects have been detected.

From an inspection of the isomer shifts it has been found that the temperature dependences of δ^{IS} for the two spin isomers are significantly different. Thus, a linear fit of the data for the low-spin $^1A_1$ constituent between 81 and 270 K gives $\partial(\delta^{IS})/\partial T = (2.5 \pm 0.3) \times 10^{-4}$ and $(4.2 \pm 0.3) \times 10^{-4}$ mm s^{-1} K^{-1} for the perchlorate and the fluoroborate complex, respectively, whereas the corresponding values for the high-spin $^5T_2$ constituent between 81 and 300 K are $(8.5 \pm 0.2) \times 10^{-4}$ and $(7.6 \pm 0.5) \times 10^{-4}$ mm s^{-1} K^{-1}. The temperature dependence of δ^{IS} is known to arise from the second-order Doppler effect.

Effective Thickness and Derived Quantities. Following the procedure outlined in the Experimental Section, we have determined the effective thickness t_i, i = $^5T_2$, $^1A_1$, for the two ground states individually. In Figure 3, the quantity $-\ln(\sum t_i)$ is plotted as a function of temperature for both $[Fe(4\text{-}paptH)_2](ClO_4)_2 \cdot 2H_2O$ and $[Fe(4\text{-}paptH)_2](BF_4)_2 \cdot 2H_2O$. The observed curvature in the transition region indicates that the Debye–Waller factors for the two constituents, $-\ln f_{^5T_2}$ and $-\ln f_{^1A_1}$, are different. It has been pointed out recently[10] that the detailed determination of $f_{^5T_2}$ and $f_{^1A_1}$ for molecular com-

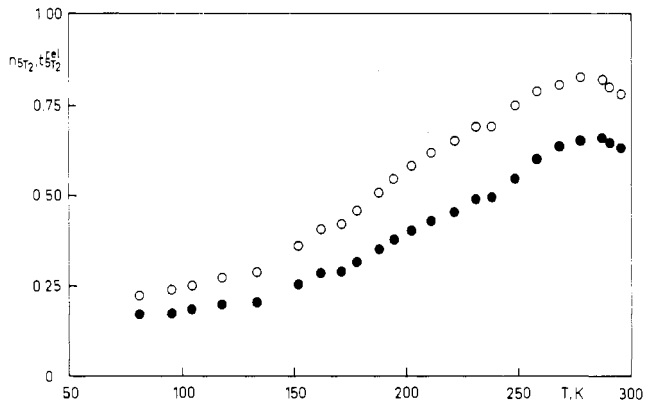

Figure 4. Temperature dependence of the relative effective thickness $t_{^5T_2}^{rel} = t_{^5T_2}/t_{total}$ for $[Fe(4\text{-paptH})_2](ClO_4)_2\cdot 2H_2O$ (●) and the derived values of the high-spin fraction, $n_{^5T_2}$ (○).

pounds is subject to certain simplifying assumptions. The iterative procedure based on the high-temperature approximation of the Debye–Waller factor (method II[10]) has been employed here to obtain the high-spin fraction, $n_{^5T_2}$. In Figure 4, both $t_{^5T_2}/t_{total}$ and $n_{^5T_2}$ are displayed as a function of temperature for $[Fe(4\text{-paptH})_2](ClO_4)_2\cdot 2H_2O$. Note that any difference between the two quantities is attributable to the difference in the recoil-free fraction of the two spin constituents (cf. eq 2). It is customary to define the transition temperature T_c for spin transitions as that temperature where $n_{^5T_2} = 0.50$. From the above results, it is found that, for $[Fe(4\text{-paptH})_2](ClO_4)_2\cdot 2H_2O$, $T_c \approx 185$ K. However, since the spin transitions studied at present are very gradual and incomplete at the two temperature limits, the value of T_c is not very informative.

For $[Fe(4\text{-paptH})_2](BF_4)_2\cdot 2H_2O$, a closely similar temperature behavior of the quantities $t_{^5T_2}/t_{total}$, $-\ln(\sum t_i)$, and $n_{^5T_2}$ was obtained. Therefore, these data are not presented in detail, except for $t_{^5T_2}/t_{total}$, which have been included in Table II. From these results, the transition temperature is found as $T_c \approx 220$ K.

Magnetic Properties. The magnetism of $[Fe(4\text{-paptH})_2](ClO_4)_2\cdot 2H_2O$ and $[Fe(4\text{-paptH})_2](BF_4)_2\cdot 2H_2O$ has been measured between 89 and 343 K for both increasing and decreasing temperatures. For the perchlorate complex, the effective magnetic moment at 303 K, $\mu_{eff} = 4.80\ \mu_B$, is indicative of a high-spin $^5T_2$ ground state with some residual low-spin $^1A_1$ contribution, whereas $\mu_{eff} = 2.22\ \mu_B$ at 89 K is consistent with a low-spin $^1A_1$ ground state with contribution of a residual $^5T_2$ fraction. For the complex tetrafluoroborate, analogous conclusions are applicable to the obtained results, viz. $\mu_{eff} = 4.57\ \mu_B$ at 303 K and $\mu_{eff} = 1.81\ \mu_B$ at 89 K. The detailed magnetic data for both $[Fe(4\text{-paptH})_2](ClO_4)_2\cdot 2H_2O$ and $[Fe(4\text{-paptH})_2](BF_4)_2\cdot 2H_2O$ are listed in Table III. An attempt has been made to determine the high-spin fraction $n_{^5T_2}$ for $[Fe(4\text{-paptH})_2](BF_4)_2\cdot 2H_2O$ on the basis of the magnetic data by employing $\mu_{eff} = 0$ and $\mu_{eff} = 5.0\ \mu_B$ for the pure $^1A_1$ and the pure $^5T_2$ ground states, respectively. The choice of these values is based on the magnetism of related complexes that do not exhibit a temperature-induced spin transition. The change in $n_{^5T_2}$ with temperature determined in this way is in reasonable agreement with the results obtained from the Mössbauer spectra (viz. method II[10]).

X-ray Powder Diffraction. X-ray diffraction patterns have been recorded for $[Fe(4\text{-paptH})_2](ClO_4)_2\cdot 2H_2O$ at various temperatures for the diffraction angles $4.5° \le \theta \le 14.0°$. In Figure 5, the diffraction patterns for the temperatures 90.0, 201, 210, and 280 K are shown. As in the spin transition in $[Fe(bts)_2(NCS)_2]$ previously studied,[10] no new peaks arise in the transition region, but rather a continuous variation in the peak positions is observed. For four well-resolved peaks the

Table III. Magnetic Data for $[Fe(4\text{-paptH})_2](ClO_4)_2\cdot 2H_2O$ and $[Fe(4\text{-paptH})_2](BF_4)_2\cdot 2H_2O$

	$[Fe(4\text{-paptH})_2](ClO_4)_2\cdot 2H_2O$		$[Fe(4\text{-paptH})_2](BF_4)_2\cdot 2H_2O$	
T, K	χ_m^{cor},[a] cgsu mol^{-1}	μ_{eff},[b] μ_B	χ_m^{cor},[a] cgsu mol^{-1}	μ_{eff},[b] μ_B
89.0	6900	2.22	4580	1.81
109.0	6110	2.30	4130	1.90
128.0	5830	2.44	4030	2.03
146.0	6180	2.69	4430	2.27
156.0			4660	2.41
166.0	6740	2.99	4910	2.55
186.0	7390	3.32	5370	2.83
196.0			5740	3.00
205.0	7950	3.61	6110	3.16
225.0	8610	3.94	6890	3.52
245.0	9170	4.24	7690	3.88
265.0	9540	4.50	8210	4.17
285.0	9540	4.66	8560	4.42
303.0	9490	4.80	8620	4.57
323.0	9230	4.88	8560	4.70
343.0	9000	4.97	8430	4.81

[a] Diamagnetic correction for $[Fe(4\text{-paptH})_2](ClO_4)_2\cdot 2H_2O$ $\chi_m^{dia} = -394 \times 10^{-6}$ cgsu mol^{-1}; for $[Fe(4\text{-paptH})_2](BF_4)_2\cdot 2H_2O$ $\chi_m^{dia} = -404 \times 10^{-6}$ cgsu mol^{-1}. [b] $\mu_{eff} = 2.828(\chi_m^{cor}T)^{1/2}$, with experimental uncertainty approximately $\pm 0.02\ \mu_B$.

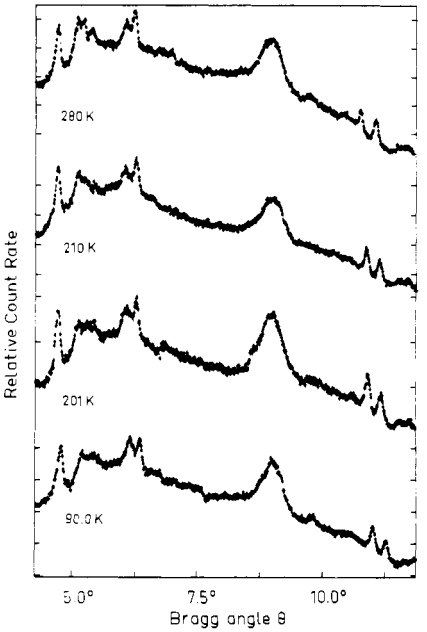

Figure 5. X-ray diffraction patterns for $[Fe(4\text{-paptH})_2](ClO_4)_2\cdot 2H_2O$ at the temperatures of 90.0, 201, 210, and 280 K.

temperature dependence was studied in detail between 90.0 and 300.0 K. In order to estimate values for peak positions and line widths, the peak profiles were fitted to individual Gaussian line shapes. For four of the reflections, i.e. those at the diffraction angles $\theta = 4.79°$ (line I), $\theta = 6.38°$ (line II), $\theta = 11.02°$ (line III), and $\theta = 11.28°$ (line IV) (values given apply for 90.0 K), the variation of the lattice spacings d_{hkl} with temperature is displayed in Figure 6. For the purpose of comparison, the figure also shows the change with temperature of the high-spin fraction $n_{^5T_2}$ as derived from the analysis of both the Mössbauer spectra and the magnetic susceptibility. Although the errors involved in the estimation of d_{hkl} values are considerable, particularly for the low angles θ, the result of interest is the observed variation of d_{hkl} values with temperature, e.g. from 9.235 Å at 90.0 K to 9.410 Å at 300.0 K for line IV. The relative accuracy of the values is sufficient to establish this result. From Figure 6 it is thus clear

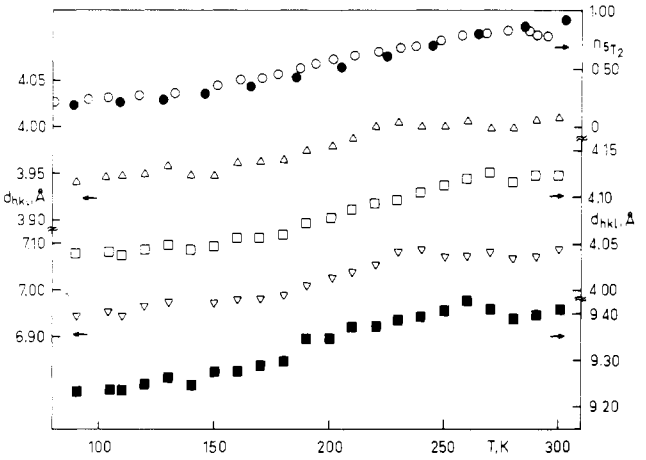

Figure 6. Temperature dependence of the lattice spacings d_{hkl} for four intense Bragg reflections of $[Fe(4\text{-paptH})_2](ClO_4)_2 \cdot 2H_2O$ at θ = 4.791, 6.376, 11.021, and 11.278° and comparison with the temperature dependence of the high-spin fraction $n_{^5T_2}$ from Mössbauer-effect (○) and magnetic susceptibility measurements (●).

that the temperature dependence of lattice spacings runs closely parallel to that of $n_{^5T_2}$. The change establishes the volume expansion which accompanies the transformation from the low-spin $^1A_1$ to the high-spin $^5T_2$ state with increasing temperature. In addition, the observations are good enough to rule out the possibility of any crystallographic phase change associated with the observed spin transition.

For $[Fe(4\text{-paptH})_2](BF_4)_2 \cdot 2H_2O$, again a continuous shift of peak positions is found as the transition is progressing. A detailed analysis of the data was not carried out, since the peaks were rather broad and less pronounced than in the perchlorate complex. It is clear, however, that the same conclusions as for the perchlorate will be applicable here.

Discussion

It is evident that the high-spin ($^5T_2$) ⇌ low-spin ($^1A_1$) transition in the compounds $[Fe(4\text{-paptH})_2](ClO_4)_2 \cdot 2H_2O$ and $[Fe(4\text{-paptH})_2](BF_4)_2 \cdot 2H_2O$ may be described in terms of a continuous change with temperature of basic physical properties, such as the ^{57}Fe Mössbauer effect, the effective magnetic moment, and the lattice spacings derived from X-ray diffraction, resulting from a gradual change in the $^5T_2$ fraction. No hysteresis effects have been observed for any of these quantities. The residual fraction of the $^5T_2$ state at low temperatures is around 0.22, and that of the $^1A_1$ state at high temperatures is approximately 0.22 as well. The transition is thus rather complete at both temperature ends.

In Figure 4, an apparent decrease in the values $t_{^5T_2}/t_{total}$ and $n_{^5T_2}$ takes place in the region of room temperature. This decrease originates from fitting uncertainties since, due to a complete superposition of the spectra in the lower velocity region and the relatively small fraction of the $^1A_1$ constituent, the estimation of the areas of the two component spectra is uncertain. The fact that the values of $-\ln(\sum t_i)$ show a continuous variation in this temperature range (cf. Figure 3) implies that the given explanation is correct.

It should be also noted that, if no difference between the Debye–Waller factors, $-\ln f_{^5T_2}$ and $-\ln f_{^1A_1}$, for the two components were involved, the temperature function of the quantity $-\ln(\sum t_i)$ should give a straight line in the high-temperature approximation. In the present study, the temperature variation of $-\ln(\sum t_i)$ for the two compounds shows a clear curvature in the region of T_c (cf. Figure 3) and thus the Debye–Waller factors are different. The important fact is that this conclusion directly follows from the areas under the Mössbauer lines and is not subject to any additional assumptions or approximations. The different Debye–Waller factors are a consequence of the different Fe–N bond distances and various other changes in the geometry[13-16] of the molecules within the two spin isomers as well as the variations of the associated vibrations. For molecular crystals, two types of vibrations are of importance: (i) intramolecular vibrations of higher frequency (optical branch); (ii) intermolecular vibrations of lower frequency (acoustical branch). In general, the Mössbauer fraction is determined predominantly by the lower energy lattice vibrations. From the results of X-ray diffraction it follows that, in the high-spin ($^5T_2$) ⇌ low-spin ($^1A_1$) transitions of the continuous type studied at present, the two spin isomers of the molecule are almost randomly distributed within the *same* lattice. Consequently, the intermolecular vibrations are expected to be similar, whereas the intramolecular vibrations will be different.[17-19] The nonlinear behavior of $-\ln(\sum t_i)$ with temperature therefore demonstrates the effect of the variation of intramolecular vibrations on the recoil-free fraction, as a result of the spin transition.

The rather significant difference observed in the temperature factors of the isomer shift also follows from the change in Fe–N bond distances accompanying the spin transition. It is well-known that the temperature-dependent contribution to the isomer shift is due to the second-order Doppler effect. The suggested difference of Debye–Waller factors for the two spin isomers is then directly supported by the different contribution of the second-order Doppler effect since, in the harmonic approximation, the two quantities are linearly related.[20]

For $[Fe(bts)_2(NCS)_2]$, anomalies of the temperature dependence of the quadrupole splitting $\Delta E_Q(^5T_2)$ and the absorber line width $\Delta\Gamma^{abs} = \Gamma_{^5T_2}{}^{abs} - \Gamma_{^1A_1}{}^{abs}$ were found,[10] which are a consequence of the different behavior of the residual high-spin $^5T_2$ fraction. For the compounds $[Fe(4\text{-paptH})_2](ClO_4)_2 \cdot 2H_2O$ and $[Fe(4\text{-paptH})_2](BF_4)_2 \cdot 2H_2O$, such anomalies are not as clearly apparent due to the very gradual and incomplete nature of the transition.

For all of the iron(II) complexes of the paptH and substituted paptH ligands, the values of the quadrupole splitting for the low-spin $^1A_1$ state have been found to be unusually large.[21,22] This result seems to be due to the unsymmetrical nature of the ligand and the expected distortion created by the tridentate coordination of the ligands at the site of the iron ion. We have performed a comparison of quadrupole splittings of the two spin states, high-spin $^5T_2$ and low-spin $^1A_1$, over an extended temperature range and for a number of complexes of the paptH and substituted paptH ligands. From the results, a systematic trend is observed such that, if on substitution in the ligand ring the value of $\Delta E_Q(^1A_1)$ increases, the corresponding value of $\Delta E_Q(^5T_2)$ decreases. However, a rational explanation for this finding cannot be offered.

The continuous variation in the X-ray diffraction patterns for the two compounds studied and for $[Fe(bts)_2(NCS)_2]$[10] contrasts with the appearance of distinct, individual patterns for the high-spin $^5T_2$ and low-spin $^1A_1$ phases in systems showing a discontinuous transition. For these, the relative intensities of the distinct patterns are strongly temperature dependent in the region of T_c. For the present compounds,

(13) König, E., Watson, K. J. *Chem. Phys. Lett.* **1970**, *6*, 457.
(14) Katz, B. A.; Strouse, C. E. *J. Am. Chem. Soc.* **1979**, *101*, 6214.
(15) Mikami, M.; Konno, M.; Saito, Y. *Acta Crystallogr., Sect. B* **1980**, *B36*, 275.
(16) Cecconi, F.; Di Vaira, M.; Midollini, S.; Orlandini, A.; Sacconi, L. *Inorg. Chem.* **1981**, *20*, 3423.
(17) König, E.; Madeja, K. *Spectrochim. Acta, Part A* **1967**, *23A*, 45.
(18) Takemoto, J. H.; Hutchinson, B. *Inorg. Nucl. Chem. Lett.* **1972**, *8*, 769.
(19) Takemoto, J. H.; Hutchinson, B. *Inorg. Chem.* **1973**, *12*, 705.
(20) Taylor, R. D.; Craig, P. P. *Phys. Rev.* **1968**, *175*, 782.
(21) Ritter, G.; König, E.; Irler, W.; Goodwin, H. A. *Inorg. Chem.* **1978**, *17*, 224.
(22) König, E.; Ritter, G.; Irler, W.; Kanellakopulos, B. *J. Phys. Chem. Solids* **1978**, *39*, 521.

intensities remain almost unchanged and no new peaks arise in the course of the transformation. However, both the peak positions and the lattice spacings derived therefrom show a temperature shift that conforms to that of the high-spin fraction $n_{^5T_2}$ (cf. Figure 6). These results may be rationalized if the distribution of the two spin isomers within the lattice is considered. Thus a single X-ray diffraction pattern will indeed be found, if a random distribution of the minority constituent within the majority phase is assumed. On the other hand, different and individual diffraction patterns for the two phases will be expected, if a narrow distribution of the minority phase, accompanied by pronounced domain formation, is assumed. This is apparently the situation that is encountered for spin transitions of the discontinuous type.

For the present compounds, and for $[Fe(bts)_2(NCS)_2]$,[10] then, a wide distribution of the minority constituent within the majority phase may be assumed. Apparently the high-spin $^5T_2$ and low-spin $^1A_1$ species together constitute a system that is akin to that of a solid solution of two components. It is not unlikely that the interpretation offered here may be applicable to all spin transitions of the continuous type. Additional investigations are in progress.

Acknowledgment. The authors appreciate financial support by the Deutsche Forschungsgemeinschaft and the Fonds der Chemischen Industrie.

Registry No. $[Fe(4\text{-paptH})_2](ClO_4)_2$, 86527-11-9; $[Fe(4\text{-paptH})_2](BF_4)_2$, 49731-99-9.

Contribution from the Research School of Chemistry, The Australian National University, Canberra, ACT 2600, Australia

Rapid Electron Self-Exchange Involving Low-Spin Cobalt(II) and Cobalt(III) in an Encapsulated Cage Complex

R. V. DUBS, L. R. GAHAN, and A. M. SARGESON*

Received November 19, 1982

The electron self-exchange rate between the Co(II) and Co(III) macrobicyclic cage complexes of azacapten (8-methyl-1,3,13,16-tetraaza-6,10,19-trithiabicyclo[6.6.6]eicosane) has been measured by the NMR line-broadening technique (k_2 = 4500 (±300) M^{-1} s^{-1} at 25 °C). The activation parameters are $\Delta H^* = 7$ (±3) kcal mol^{-1} and $\Delta S^* = -18$ (±11) cal deg^{-1} mol^{-1}. The magnetic moments for the Co(II) complex are slightly different in the crystal lattice (1.89 μ_B) and solution (2.35 μ_B), but both indicate the Co(II) ion is largely in the low-spin condition ($t_{2g}^6e_g^1$). The large rate constant is consistent with this low-spin condition in both the Co(II) and the Co(III) ions and the consequently reduced bond lengths and therefore reduced reorganization energy relative to those of the $Co(NH_3)_6^{2+/3+}$, $Co(en)_3^{2+/3+}$, and $Co(sep)^{2+/3+}$ ions.

Introduction

The chemistry of a number of complexes in which cobalt(III) and cobalt(II) ions are effectively encapsulated within a macrobicyclic ligand framework has been reported previously.[1-3] The tightly bonding nature of these cage ligands ensures the nonlability of the cobalt(II) species. In fact, it is possible to isolate chiral cobalt(II) cage complexes.[1-3] Two such macrobicyclic cage systems are the octaaza $[Co(sep)]^{3+/2+}$ (**1**)[1] and the nitrogen–sulfur $[Co(azacapten)]^{3+/2+}$ (**2**)[3] complexes.

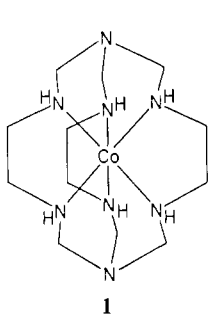

1

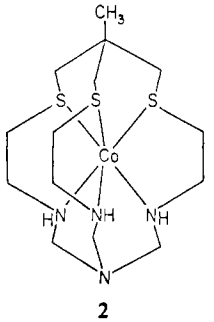

2

The inert octahedral nature of these and other similar cage complexes ensures that reactions involving the cobalt(II) species occur in the absence of ligand–metal exchange.[1-3] As a consequence, a reaction involving the exchange of an electron between the Co(II) and Co(III) states must occur via a pathway not involving ligand exchange and presumably follows an outer-sphere path (eq 1).[4]

$$*Co(azacapten)^{3+} + Co(azacapten)^{2+} \rightleftharpoons *Co(azacapten)^{2+} + Co(azacapten)^{3+} \quad (1)$$

The electron self-exchange rates of a series of such complexes have been studied previously with use of a polarimetric technique.[5,6] A preliminary investigation of the sulfur–nitrogen cage indicated a rate of self-exchange too rapid to be measured by this method. The present paper explores measurements of the electron-transfer rate by an NMR line-broadening technique.

Experimental Section

All manipulations involving solutions of the cobalt(II) complexes were performed under an atmosphere of nitrogen that had been scrubbed with solutions of Cr^{2+}. Aqueous solutions of the oxygen-sensitive cobalt(II) complexes were transferred under a positive pressure of oxygen-free nitrogen with stainless steel transfer tubing.

Commercial CF_3SO_3H (3M Co.) was distilled before use.

^1H NMR spectra were recorded in D_2O solution relative to sodium 2,2-dimethyl-2-silapentane-5-sulfonate (DSS) as an internal standard, except as described.

$[Co(azacapten)]Cl_3$ was prepared as described previously[3] and isolated as its triflate ($CF_3SO_3^-$) salt with use of CF_3SO_3H. The

(1) Creaser, I. I.; Harrowfield, J. M.; Herlt, A. J.; Sargeson, A. M.; Springborg, J.; Geue, R. J.; Snow, M. R. *J. Am. Chem. Soc.* **1977**, *99*, 1381. $[Co(sep)]^{3+}$ is the macrobicyclic ion [(1,3,6,8,10,13,17,19-octaazabicyclo[6.6.6]eicosane)cobalt(III)](3+).
(2) Creaser, I. I.; Geue, R. J.; Harrowfield, J. M.; Herlt, A. J.; Sargeson, A. M.; Snow, M. R. *J. Am. Chem. Soc.* **1982**, *104*, 6016.
(3) Gahan, L. R.; Hambley, T. W.; Sargeson, A. M.; Snow, M. R. *Inorg. Chem.* **1982**, *21*, 2699.
(4) Basolo, B.; Pearson, R. G. "Mechanism of Inorganic Reactions", 2nd ed.; Wiley: New York, 1967; p 455.
(5) Dwyer, F. P.; Sargeson, A. M. *J. Phys. Chem.* **1961**, *65*, 1892.
(6) Creaser, I. I.; Sargeson, A. M.; Springborg, J.; Zanella, A. *Inorg. Chem.*, in press.

0020-1669/83/1322-2523$01.50/0